ARTICLE
Journal of Cellular Biochemistry 109:498–508 (2010)

Journal of Cellular Biochemistry

PPAR-β Facilitating Maturation of Hepatic-Like Tissue Derived From Mouse Embryonic Stem Cells Accompanied by Mitochondriogenesis and Membrane Potential Retention

Dan-yan Zhu,* Jia-ying Wu, Huan Li, Jie-ping Yan, Mei-yuan Guo, Yan-bo Wo, and Yi-jia Lou*

Institute of Pharmacology, Toxicology and Biochemical Pharmaceutics, Zhejiang University, Hangzhou 310058, China

ABSTRACT

Relatively little is known about mitochondria metabolism in differentiating embryonic stem (ES) cells. Present research focused on several elements of cellular energy metabolism in hepatic-like tissue derived from mouse ES cells. We demonstrated that mitochondrial location patterns and mitochondrial membrane potential ($\Delta\Psi_m$) existed in subsequent differentiation of the tissue. Mitochondriogenesis appeared at the early stage and kept a normal $\Delta\Psi_m$ in differentiated mature hepatocytes. Peroxisome proliferator-activated receptor-α (PPAR-α) expression was transitorily increased at the beginning, and kept a relatively low level later, which accompanied by expression of PPAR-γ coactivator (PGC)-1α, a master regulator of mitochondrial biogenesis. PPAR-β expression showed robust up-regulation in the late differentiation course. Enhanced co-expressions of PPAR-β and albumin with catalysis of UDP-glucuronosyltransferases (UGTs) were observed at mature stage. While PPAR-γ expression changed little before and after differentiation. Mitochondriogenesis could be accelerated by PPAR-α specific agonist WY14643 and abolished by its antagonist GW6471 at the early stage. Neither of them affected mitochondrial $\Delta\Psi_m$ and albumin generation in the differentiated hepatocytes. Furthermore, maturation of hepatic-like tissue and mitochondriogenesis in hepatocyte could be efficiently stimulated by PPAR-β specific agonist L165041 and abolished by PPAR-β specific antagonist GSK0660, but not affected by PPAR-γ specific agonist GW1929. In conclusion, the derived hepatic tissue morphologically possessed cellular energy metabolism features. PPAR-α seemed only necessary for early mitochondriogenesis, while less important for $\Delta\Psi_m$ retention in the mature tissue derived. The stimulation of PPAR-β but not -γ enhanced hepatogenesis, hepatocytes maturation, and mitochondriogenesis. PPAR-β took an important role in cellular energy metabolism of hepatogenesis. J. Cell. Biochem. 109: 498–508, 2010.

KEY WORDS: PEROXISOME PROLIFERATOR-ACTIVATED RECEPTOR (PPAR-α; -β/δ; AND -γ); MITOCHONDRIOGENESIS; MITOCHONDRIAL MEMBRANE POTENTIAL ($\Delta\Psi_M$); HEPATOGENESIS; EMBRYONIC STEM CELLS

Mitochondria are organelles responsible for the production of the vast majority of ATP within eukaryotic cells. It has been reported that human embryonic stem (ES) cells have very few and small mitochondria with very simple cristae, whereas differentiated cells gain a normal organelle phenotype with more and regular mitochondria, together with an increase in ATP production [Oh et al., 2005; Cho et al., 2006]. Mitochondriogenesis is an adaptive biological process that occurs in response to developmental and physiologic cues. The hepatic tissue derived from ES cells in vitro, faithfully recapitulates the process in vivo. It has been considered as an efficiency model in metabolism, drug discovery, and even in inflammation and cytoprotection research [Tsutsui et al., 2006; Monica et al., 2007; Zhu et al., 2008]. So far, however, few researchers consider mitochondriogenesis and mitochondrial function involved in ES cells differentiation [Lonergan et al., 2007], including hepatic tissue derived. Present research focused on several elements of cellular energy metabolism in hepatic-like tissue derived from mouse ES cells.

Prior to embryo implantation in vivo, embryonic cells are contained in a hypoxic environment within the uterine lumen. The embryonic cells rely on anaerobic metabolism to meet their energy demands. It is therefore not surprising that ES cells have few mitochondria that lack cristae development. It has been shown that ATP content of blastomeres is correlated to their mitochondrial

Grant sponsor: National Natural Sciences Foundation of China; Grant numbers: 30672564, 30600762, 30873068, 30472112, 30171121, 30070904; Grant sponsor: Zhejiang Provincial Natural Science Foundation of China; Grant number: Y206473.

*Correspondence to: Prof. Dr. Yi-jia Lou and Dr. Dan-yan Zhu, Institute of Pharmacology, Toxicology and Biochemical Pharmaceutics, Zhejiang University, Hangzhou 310058, China. E-mail: yijialou@zju.edu.cn, zdyzxb@zju.edu.cn

Received 24 August 2009; Accepted 21 October 2009 • DOI 10.1002/jcb.22426 • © 2009 Wiley-Liss, Inc.
Published online 8 December 2009 in Wiley InterScience (www.interscience.wiley.com).

content [Brown, 1992; Squirrell et al., 2003; Bavister, 2006; Lonergan et al., 2006]. The magnitude of the inner mitochondrial membrane potential, or its polarity ($\Delta\Psi_m$), is a physiochemical property of mitochondria related to levels of organelle activity, and differences in the magnitude and spatial distribution of high- and low-polarized mitochondria have been suggested to influence early embryo competence [Van Blerkom et al., 2002; Van Blerkom, 2004]. Analysis of $\Delta\Psi_m$ may be a means by which differential mitochondrial activity or regulatory function(s) can be investigated in living pre-implantation-stage embryos, especially with respect to domains of high- and low-polarized organelles [Van Blerkom, 2004].

Mitochondrial biogenesis requires coordinated changes in the metabolic enzymes of oxidative phosphorylation, TCA cycle, and fatty acid oxidation. Peroxisome proliferator-activated receptors (PPARs) are lipid-activatable transcription factors that belong to the nuclear hormone receptor superfamily. Three PPAR isotypes, PPAR-α, PPAR-β, and PPAR-γ have been distinguished by tissue- and developmental-specific patterns of expression [Willson et al., 2000]. The differential expression and activation of PPARs during rat and mouse embryonic development, suggest that a period of PPARs exposure may be critical to normal development [Kliewer et al., 1994; Braissant and Wahli, 1998; Steinmetz et al., 2005]. However, the isotype expressions in specific tissue during development, such as embryonic liver, have not been investigated yet so far. PPAR-α is mainly rich in tissues that have high-energy demands, such as heart, liver, kidney, and stomach mucosa [Sher et al., 1993; Kliewer et al., 1994; Auboeuf et al., 1997]. It has also been shown to serve as a key transcriptional regulator of the energy metabolic pathway [Leone et al., 1999]. As an important coactivator of PPAR-α, PGC-1α (PPAR-γ co-activator 1α) plays an important role in energy metabolism by coordinating transcriptional programs of mitochondrial biogenesis [Wu et al., 1999], adaptive thermogenesis and fatty acid β-oxidation. PPAR-β is the most ubiquitously expressed and appears very early during embryogenesis [Kliewer et al., 1994]. The relative expression of PPAR-β showed the strongest in liver, colon, and intestine, and weak in adult mouse heart. PPAR-β signaling contributes to enhanced proliferation of hepatic stellate cells [Hellemans et al., 2003]. In addition, PPAR-β has been linked to the embryo implantation. PPAR-β knockout embryos have placental defects and a substantial proportion of the embryos die in mid-gestation [Lim and Dey, 2000; Nadra et al., 2006]. Even though its other physiological and pathophysiological roles of PPAR-β are less clear [Han et al., 2005]. PPAR-γ is found primarily in the adipose tissue and has an important role in adipose differentiation [Chawla et al., 1994].

It has been reported that three isoforms are expressed in ES cells already at early stages of cardiac differentiation [Schmelter et al., 2006; Ding et al., 2007; Sharifpanah et al., 2008]. The stimulation of PPAR-α but not PPAR-β and -γ enhances cardiomyogenesis using a pathway that involves ROS and NADPH oxidase activity [Sharifpanah et al., 2008]. So far, few evidence deals with the elements of cellular energy metabolism of the ES cell-derived hepatic tissue system. The present study aimed to elucidate the magnitude and spatial distribution of high- and low-polarized mitochondria and PPARs expressions during either hepatogenesis or functional mature hepatic-like tissue from mouse ES cells.

MATERIALS AND METHODS

CELL CULTURE AND TREATMENT

The ES-D3 cells (American Type Culture Collection, CRL-1934) were differentiated into hepatic tissue as described previously [Zhu et al., 2008]. In brief, cultures of differentiating mouse ES cells were established by the formation of EB in hanging drop cultures. Drops (30 μl) containing about 600 ES cells were placed on the lids of Petri dishes, and then cultivated in hanging drops for 5 days, then EBs were plated onto gelatin-coated culture plates. D 1 referred to the day of EB plating culture in the experiment. EB was observed with light microcopy until D 18.

To investigate whether PPAR agonist or antagonist would affect the liver-genesis of ES cells, EBs were treated from plating day with either PPAR-α agonist WY14643 (6.3×10^{-6} mol/L, Sigma), PPAR-β agonist L165,041 (1×10^{-5} mol/L, Sigma), PPAR-γ agonist GW1929 (1×10^{-5} mol/L, Sigma), or PPAR-α antagonist GW6471(1×10^{-6} mol/L, Sigma) [Sharifpanah et al., 2008], PPAR-β specific antagonist GSK0660 (1×10^{-8} mol/L, Sigma) [Shearer et al., 2008].

MITOCHONDRIAL MEMBRANE POTENTIAL ($\Delta\Psi_m$) ASSAY

The fluorescent dye 5,5′,6,6′-tetrachloro-1,1′,3,3′ tetraethyl-benzimidazolylcarbocyanine iodide (JC-1; Molecular Probes, Sigma) was used to assess $\Delta\Psi_m$ in the cells. It is a lipophilic, cationic molecule that cross the mitochondrial membrane and accumulate in the negatively charged mitochondrial matrix in a potential dependent manner, with fluorescence detectable by fluorescence microscopy. At the high concentrations achieved in polarized mitochondria, JC-1 molecules form aggregates with a different fluorescence peak than the dilute dye. Cells were incubated in 0.3 μg/ml JC-1 for 30 min, rinsed, and observed in both red and green channels with a Leica DMIL fluorescence microscope. The green fluorescence channel represents the overall loading of JC-1, while the red channel represents the shift in fluorescence that occurs with the potential dependent formation of J-aggregates at high JC-1 concentrations in the mitochondrial membranes, indicated by a fluorescence emission shift from green (525 ± 10 nm) to red (610 ± 10 nm). Red fluorescence indicates active mitochondria with high $\Delta\Psi_m$ through the formation of J-aggregates. Green fluorescence is representative of JC-1 remaining in its monomeric form in less active mitochondria with low $\Delta\Psi_m$ [St John et al., 2005]. Mitochondria depolarization is specifically indicated by a decrease in the red to green fluorescence intensity ratio [Zuliani et al., 2003]. A brightfield image was taken along with each set of fluorescence images for alignment, quality control, and display purposes. Mitochondria with red fluorescence represent mature and normal function [Lee et al., 2000]. The number of cells with red fluorescence was counted as the mitochondrial numbers quantified using the bio-imaging system.

IMMUNOCYTOCHEMICAL ANALYSIS

Albumin and PPAR-α, -β, -γ expressions were detected as follows. The cells were fixed with cold methanol for 10 min. After treatment with fetal calf serum for 30 min, specimens were incubated at 4°C overnight together with the primary antibody:

polyclonal anti-albumin, polyclonal anti-PPAR-α, -β, -γ (1:50 dilution, Santa Cruz Biotechnology, CA). Then the specimens were incubated with the fluorescent antibody fluorescein isothiocyanate isomer I (FITC)-conjugated affinity-purified anti-goat IgG (1:200 dilution, Santa Cruz Biotechnology) for albumin, Rhodamine conjugated affinity purified anti-rabbit IgG (1:300 dilution, Rockland) for PPAR-α, -β, -γ 1.5 h 37°C. After double-label immunocytochemistry, 4,6-Diamidino-2-phenylindole (DAPI, Sigma–Aldrich, St. Louis, MO) was dyed for cellular nucleus. Then the cells were observed under a fluorescence microscope (Leica DMIL, German). Several visual fields were randomly selected and counted for each sample.

FLOW CYTOMETRY

EBs were harvested at D 18 and digested into single cells by 0.2% collagenase and trypsin treatment before immunostaining. Then, the cells were fixed in 4% paraformaldehyde for 60 min. After treatment with fetal calf serum for 30 min, specimens were incubated at 4°C overnight together with the primary antibody: polyclonal anti-albumin (1:50 dilution, Santa Cruz Biotechnology). Then, the cells was washed with PBS and followed by incubation with the appropriate secondary antibody: PE Conjugated Swine anti-Goat IgG (1:500) for 1 h. A total of 10,000 events were routinely collected with a FACS flowcytometer (Becton-Dickson). Differentiation was determined by comparing the fluorescence intensity of the treated cells to that of untreated cells obtained from a solvent control plate. The results were expressed as the percentage of the fluorescence intensity.

REAL-TIME RT PCR

Total RNA was extracted from ES cells, EBs, hepatic tissue derived from EBs on day 6, 12, 18 after plating (D 6, D 12, and D 18), and liver obtained from neonatal mouse, using the Trizol reagent (Gibco, BRL) in accordance with the manufacturer's instructions. The reverse transcription reactions and polymerase chain reactions were done as described previously [Zhu et al., 2008]. The sense and antisense primers designed by using Primer 3.0 software were as follows (Table I) [Sharifpanah et al., 2008]. And cDNA synthesis was performed using 3 μg RNA with MMLV RT (Invitrogen). Primer concentration for PCR was 10 pM. Amplifications were performed in a Mastercycler ep Realplex (Eppendorf, Germany) using iQTM SYBR Green Supermix (Biorad). Following programs were used: Cycle 1: Step 1: 95°C for 3 min. Cycle 2: Step 1: 95°C for 45 s; Step 2: specific annealing temperatures for 45 s; Step 3: 72°C for 30 s. Cycle 3: Step 1: 72°C for 10 min. Annealing temperatures were: 60.5°C for PPAR-α, 59°C for PPAR-β, 61°C for PPAR-γ. C_T values were automatically obtained. The amount of gene was calculated and normalized by the standard curve. Relative expression values were obtained by the amount of the tested genes in comparison with the amount of the housekeeping genes.

For semi-quantitative RT-PCR, the total RNA extracted was denatured for 3 min at 94°C, followed by the amplification in the reaction with Ampli Taq DNA polymerase: 45 s denaturation and 45 s elongation at 72°C. PCR products were analyzed by 1.5% agarose gel electrophoresis, visualized with ethidium bromide staining, and then quantified using a bio-imaging analyzer (Bio-Rad, USA). The density of the products was quantitated using Quantity One version 4.2.2 software (Bio-Rad).

WESTERN BLOT

Proteins were isolated from ES cells, EBs and hepatic tissue derived from EB on D 6, D 12, D 18, liver and heart obtained from neonatal mouse. Cells or tissues were collected in RIPA buffer and lysed 30 min on ice. Samples were clarified by centrifugation for 30 min at 13,000*g* at 4°C. An aliquot of 80 μg of the supernatant protein from each sample separated electrophoretically on a 10% SDS–polyacrylamide gel. Subsequently, proteins were transferred onto 0.22-μm pore size nitrocellulose membranes for 90 min and blocked overnight, followed by an overnight incubation at 4°C with respective antibody. The primary antibodies used included rabbit polyclonal anti-PPAR-α, -β, -γ, goat polyclonal anti-PGC-1α, goat polyclonal anti-OCT-4, goat polyclonal anti-albumin at 1:500 dilution, GAPDH primary antibody at 1:10000 dilution (Santa Cruz Biotechnology). Then the membranes were incubated with peroxidase-conjugated affinipure goat anti-rabbit IgG or with horseradish peroxidase HRP-Conjugated rabbit anti-goat antibody at 1:5,000 dilution (Affinity Bioreagents, Golden, CO). The proteins were visualized autoradiographically with an enhanced chemiluminescent substrate (ECL, Pierce, USA), and scanned using a bio-imaging analyzer (Bio-Rad). The density of the products was quantitated using Quantity One version 4.2.2 software (Bio-Rad).

UDP-GLUCURONOSYLTRANSFERASES (UGTs) ACTIVITY ASSAY

Microsomes were prepared from ES cells, 18-day-old hepatic-like tissue, and mouse adult liver [Shi and Lou, 2005]. 7-Hydroxyl-4-trifluoromethyl coumarin (7-HFC) glucuronide formation was confirmed by HPLC after incubation with or without microsomes of hepatic-like tissue in vitro. 7-HFC (Sigma, USA) was added as a substrate into the incubation solution (50 mmol/L Tris–HCl, 10 mmol/L $MgCl_2$, 8.5 mmol/L saccharolactone, 0.02 g/L

TABLE I. Primers and Conditions for Semiquantitative and Real-Time RT-PCR

Genes	Primers	Size (bp)	Annealing temperature (°C)	Cycles
PPAR-α	5′-GGCTGTAAGGGCTTCTTT-3′ 5′-CAGGTAGGCTTCGTGGAT-3′	130	60.5	40
PPAR-β	5′-TTGAGCCCAAGTTCGAGTTTG-3′ 5′-CGGTCTCCACACAGAATGATG-3′	100	59	30
PPAR-γ	5′-CCACCAACTTCGGAATCTGCT-3′ 5′-TTTGTGGATCCGGCAGTTAAGA-3′	412	61	30
GAPDH	5′-TCCATGCCATGACTGCCACTC-3′ 5′-TGACCTTGCCCACAGCCTTG-3′	212	58	35

alamethicin) and 2 mg/L microsomal homogenate. After pre-incubation at 37°C for 5 min, 0.5 μmol UDP-glucuronic acid (UDPGA) was added as a cofactor to start the reaction. The enzymatic reaction was stopped by adding ice-cold acetonitrile at 37°C in a shaking water bath, then, it was centrifuged at 16,000*g* for 20 min. A 20 μL aliquot of the supernatant was analyzed by reversed phase RP-HPLC (Shimadzu LC-10ATvp; Kyoto, Japan LC-10AT pump, a SPD-10A UV detector and a zorbax ODS-C18 column). The mobile phase consisted of 10 mmol/L KH_2PO_4 adjusted to pH 3.0 with 0.5% triethylamine and 90% acetonitrile, was operated at a constant flow rate (1 ml/min) and the metabolite was detected at 325 nm. The gradient was 30% acetonitrile initial, followed by a rapid increase to 65% acetonitrile in 8 min, 15 min at 30%, and a re-equilibrium at 30% acetonitrile. Following the analysis, the concentrations of glucuronides were calculated based on UV detection and a standard linear curve.

STATISTICAL ANALYSIS

Data are expressed as mean values ± standard deviation (SD). At least three independent experiments were done. Statistical analysis was performed by one-way ANOVA. A value of $P < 0.05$ was considered to be significant.

RESULTS

MORPHOLOGICAL AND FUNCTIONAL MATURE HEPATIC-LIKE TISSUE

Apparent cell morphological changes have been described previously [Zhu et al., 2008] during the hepatic tissue differentiated from ES cells (Fig. 1Aa–d). Some of these albumin positive cells were binuclear, which is a characteristic of mature hepatocytes [Ogawa et al., 2005] (Fig. 1Ae,f).

The ES cell-derived hepatic tissue system had a capacity for glucuronic acid conjugation reactions by HPLC (Fig. 1B). UGTs activity of microsomes was 0.445 nmol/min/mg protein in 18-day-old hepatic-like tissue compared with 0.069 nmol/min/mg in ES cells and 2.820 nmol/min/mg in mouse adult liver (Fig. 1C).

MITOCHONDRIOGENESIS AND POLARITY ($\Delta\Psi_m$)

ES cells had the lowest mitochondrial mass and emitted almost only green fluorescence. When EBs were formed and digested, single cell stained both red and green fluorescence. Red fluorescence indicates active mitochondria with high $\Delta\Psi_m$ through the formation of J-aggregates. Green fluorescence is representative of JC-1 remaining in its monomeric form in less active mitochondria with low $\Delta\Psi_m$. The persistence of both fluorescences demonstrated the presence of both high and low $\Delta\Psi_m$ coexisted inside EBs. Within this multicellular arrangement in EB outgrowths, there was an increase in active mitochondria mass with high $\Delta\Psi_m$ in red fluorescence from D 6 to D 18 during hepatic tissue differentiation (Fig. 2A). On D 18, red fluorescence was almost observed all over the visual fields. It indicated that mitochondriogenesis started at EB formation, and the normal mitochondrial $\Delta\Psi_m$ was kept in the mature hepatic tissue on D 18.

CO-EXPRESSIONS OF PPARs AND ALBUMIN

All PPAR isoforms mRNA were expressed with different patterns. Expression of *PPAR-α* gene significantly increased from ES cells and reached maximum expression on D 6 after the plating differentiation culture. However, from D 12 to D 18, *PPAR-α* mRNA took on a down-regulating trend. *PPAR-β* mRNA expression exerted an elevated tendency during hepatic-like tissue development. While inclined form, *PPAR-γ* mRNA expression appeared low level and changed little before and after differentiation (Fig. 2B).

PPAR-α, -β, -γ proteins were all examined in ES cells and changed differently during the differentiation course. The maximum of PPAR-α protein expression was observed on D 6 and the level relatively declined from D 12. PGC-1α was increased from ES cells to EB differentiating D 12, and declined on D 18. PPAR-β protein expression decreased in EB then had an up-regulating trend by degrees with the maturation of hepatic tissue. The expression of PPAR-γ protein was also low and changed little. The protein expressions of undifferentiating marker OCT-4 and mature marker albumin [Ogawa et al., 2005; Tsutsui et al., 2006] were consistent with both morphologically or functionally in D 18 hepatic-like tissue (Fig. 2C).

On the other hand, we further investigated the relationship between the expressions of PPARs and albumin at mature hepatic tissue in situ. The results showed that PPAR-α, -β, -γ proteins were also positively detected in the albumin positively stained cells differentiated from ES cells on D 18. The fluorescence of PPAR-β was stronger than that of PPAR-α, while PPAR-γ showed less fluorescence. The fluorescence merged area of PPAR-β with albumin was the largest. The co-expressions of PPARs with albumin in the cells derived further confirmed that only PPAR-β occupied the major position in energy metabolism of hepatocytes on D 18 (Fig. 2D).

PPARs AGONISTS OR ANTAGONISTS AFFECTING LIVER MATURATION, MITOCHONDRIOGENESIS AND $\Delta\Psi_m$

Treatment with PPAR-β agonist L165041 significantly increased the fluorescence of albumin-positive cells in EB on D 18. PPAR-β agonist increasing the red fluorescence areas of hepatocytes in EB was approximately 50% evaluated by computer-assisted image analysis of albumin-positive cell areas. While the selective antagonist GSK0660 for PPAR-β decreased the level of albumin expression (Fig. 3). The results of flow cytometry showed 11% of the total cell populations were albumin positive in DMSO control group on day 18 of culture. Meanwhile, the albumin-positive cells in EBs significantly increased to 19% by the treatment of PPAR-β agonist L165041 compare with control. However, PPAR-β antagonist GSK0660 obviously lowered to reach 5% of the albumin-positive cells. On the other hand, PPAR-α agonist WY14643 or antagonist GW6471, as well as PPAR-γ agonist GW1929 showed no conspicuous effects on the albumin expression on the phase of mature hepatic cells formation, which was determined by both immunocytochemistry assay and flow cytometry analysis (Fig. 3). Since PPAR-γ expression kept low level and remained unchanged until on D 18, we did not consider to use its antagonist either.

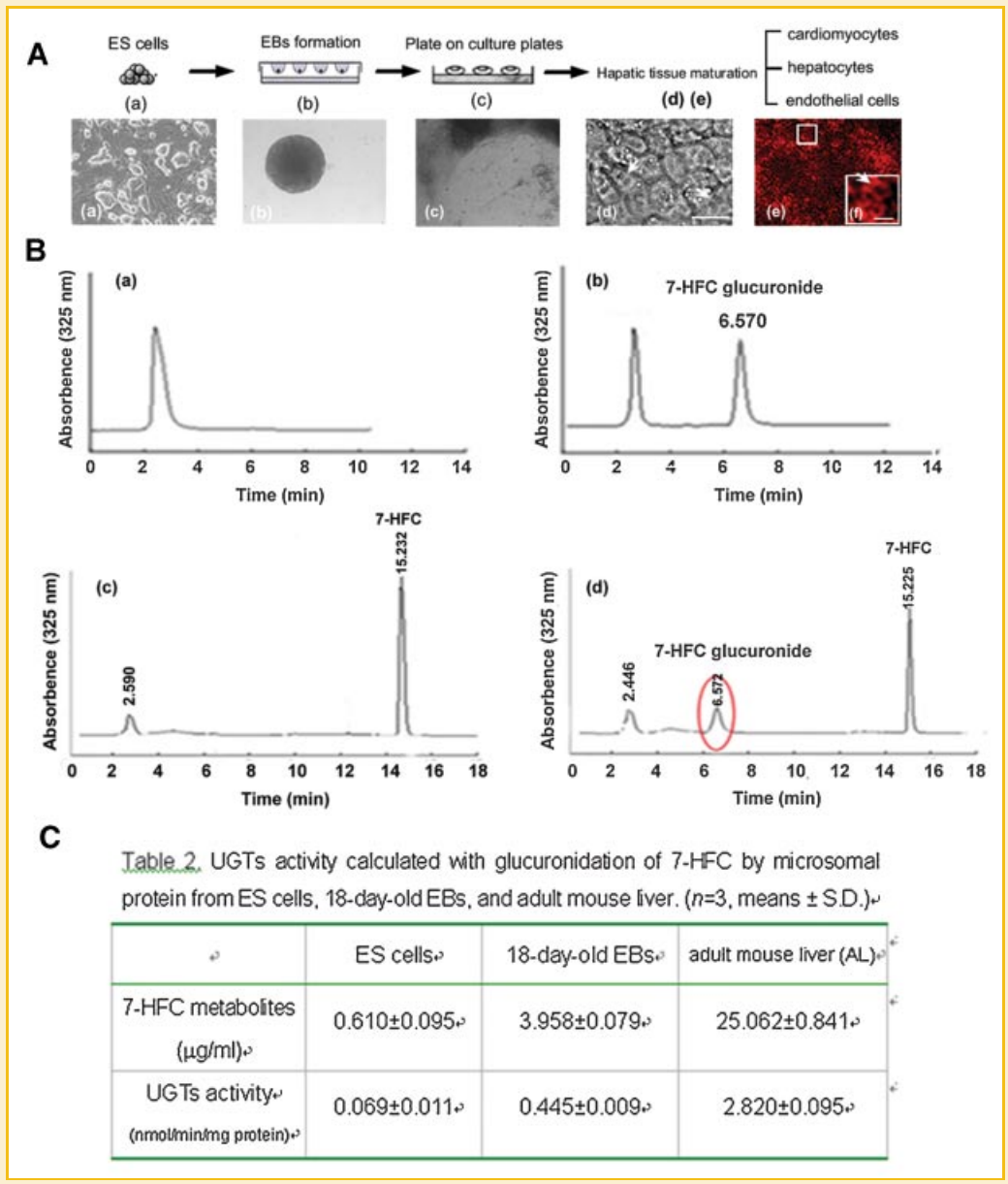

C

Table 2. UGTs activity calculated with glucuronidation of 7-HFC by microsomal protein from ES cells, 18-day-old EBs, and adult mouse liver. (n=3, means ± S.D.)

	ES cells	18-day-old EBs	adult mouse liver (AL)
7-HFC metabolites (μg/ml)	0.610±0.095	3.958±0.079	25.062±0.841
UGTs activity (nmol/min/mg protein)	0.069±0.011	0.445±0.009	2.820±0.095

Fig. 1. Apparent cell morphological changes, and metabolic function of the ES cell-derived hepatic tissue. A: Schematic representation of the differentiation protocol. A(a) Colonies of ES cells on a feeder layer of mouse embryonic fibroblasts, (b) EB formation, (c) EB within 18 days after plating onto a gelatinous layer, (d) the binuclear marker (arrows) for mature hepatic cells in the outgrowths of EB, (e) a cluster of albumin-positive binuclear cells (red, arrow) in the multilayered structure. The rectangular frames indicate the part magnified in panel (f). B: HPLC demonstrating the catalytic activity of UGTs. B(a) Blank cell homogenate, (b) cell homogenate containing 7-HFC glucuronide, (c) with substrate of 7-HFC and UDPGA without cell homogenate, (d) reacting with substrate of 7-HFC and UDPGA in the derived mature hepatocytes homogenate. C: UGTs activity calculated with glucuronidation of 7-HFC by microsomal protein from ES cells, 18-day-old EBs, and mouse adult mouse liver. Bar = 100 μm (Aa–c), 50 μm (Ae), 10 μm (Ad,f). [Color figure can be viewed in the online issue, which is available at www.interscience.wiley.com.]

PPAR-α agonist WY14643 or antagonist GW6471 failed to keep mitochondrial $\Delta\Psi_m$ on the later period of hepatic differentiation, although WY14643 and GW6471 did accelerate or disrupt the mitochondriogenesis during the early differentiation. Moreover, mitochondriogenesis during the differentiation of EBs and mitochondrial $\Delta\Psi_m$ retain could be efficiently stimulated by the specific PPAR-β agonist L165041 and prevented by PPAR-β antagonist GSK0660 in the period of mitochondriogenesis. Whereas, the specific PPAR-γ agonist GW1929 showed no effects on the mitochondrial $\Delta\Psi_m$ (Fig. 4).

DISCUSSION

It is becoming increasingly apparent that mitochondria are involved in the establishment of developmental competence. The differences

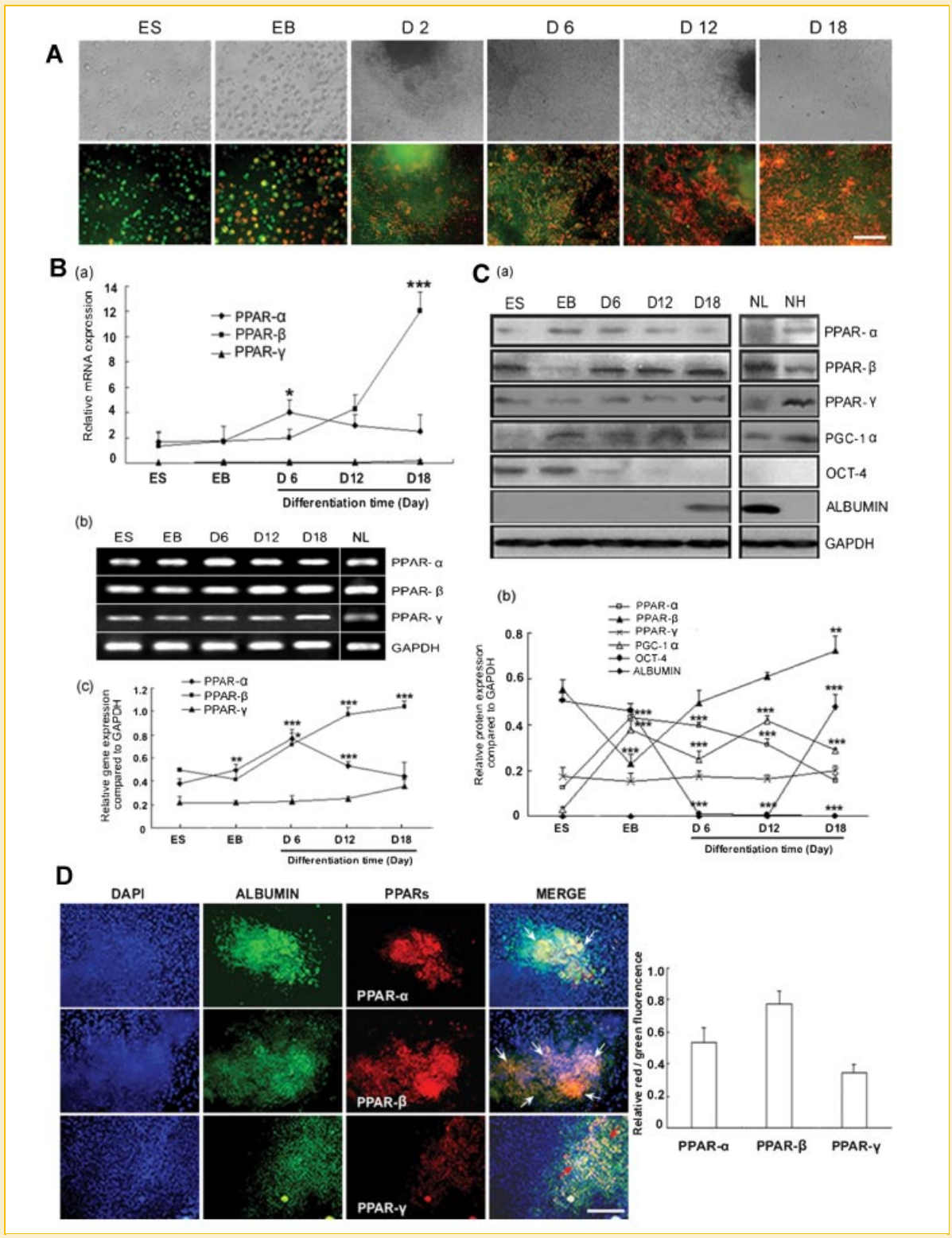

Fig. 2. High mitochondrial membrane potential ($\Delta\Psi_m$) formation and co-expressions of PPARs and albumin in the hepatic tissue differentiated from ES cells. A: Phase contrast and immune micrographs for the change $\Delta\Psi_m$. The samples were the digested ES cells, EBs, plating EBs differentiated on D 2, D 6, D 12, D 18. B(a) Quantity analysis of *PPAR-α*, *PPAR-β*, and *PPAR-γ* mRNA levels in relation to *GAPDH* identified by real-time PCR during the hepatic tissue differentiating course, (b) RT-PCR products for *PPARs* genes, (c) data plotted for *PPAR-α*, *PPAR-β* and *PPAR-γ* genes in relation to *GAPDH* gene. C(a) Western blot analysis of PPARs proteins expressions, neonatal mouse liver (NL), neonatal mouse heart (NH), (b) data plotted for PPARs proteins in relation to GAPDH. D: Co-localization of PPARs and albumin in the hepatic tissue on D 18. The arrows indicate the co-expressions of PPARs and albumin in the hepatocytes. DAPI staining showed the location. Data plotted for *PPAR-α*, *PPAR-β* and *PPAR-γ* (red) fluorescence compared with albumin (green) fluorescence. Bar = 25 μm (A-ES, EB), 50 μm (A-D 2 to D 18, D). Similar data were obtained in three independent experiments at least. $^{*}P < 0.05$, $^{**}P < 0.01$, $^{***}P < 0.001$ versus ES cells. [Color figure can be viewed in the online issue, which is available at www.interscience.wiley.com.]

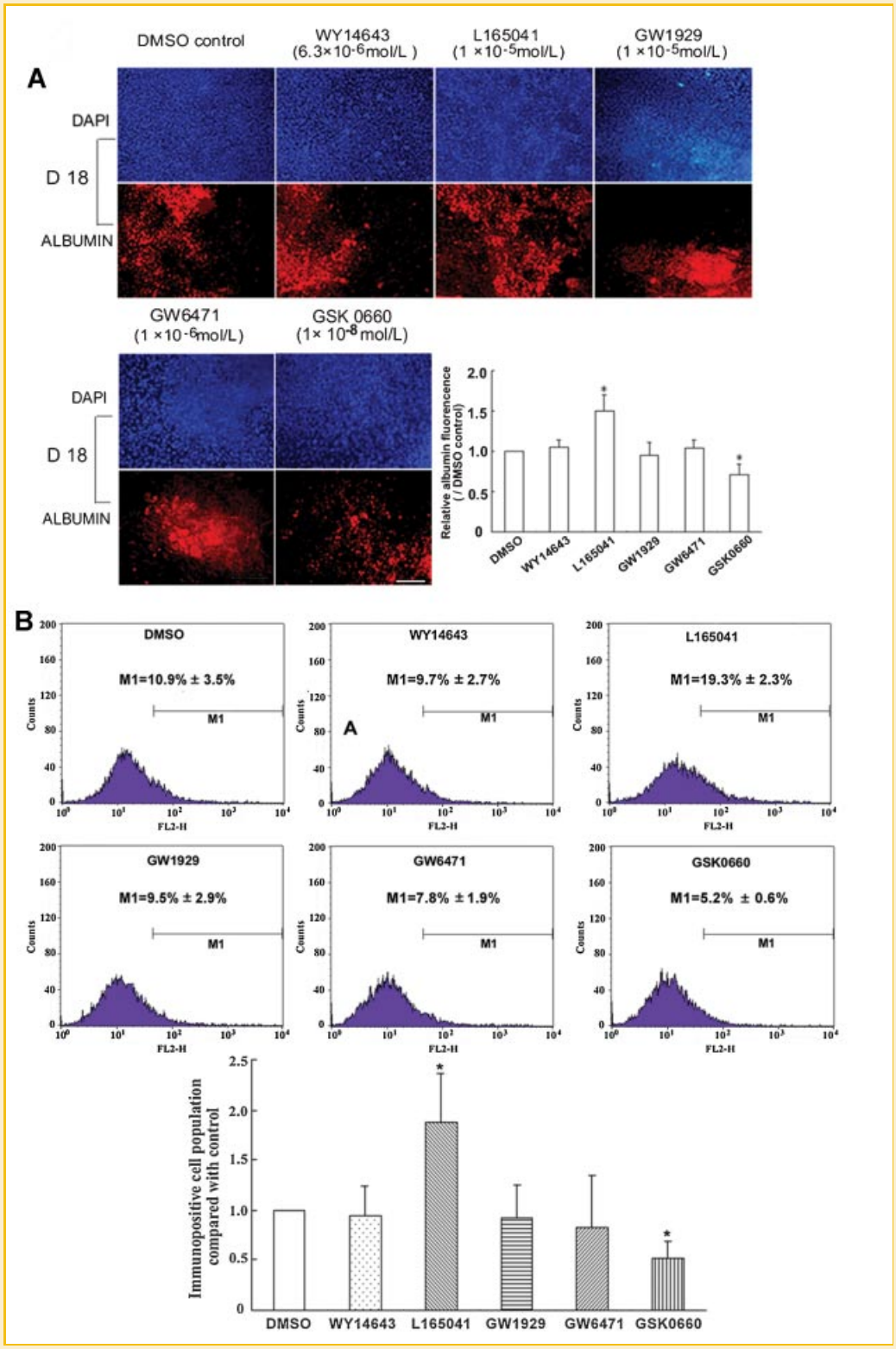

Fig. 3. Effects of PPARs agonists or antagonists on albumin expression in the ES cell-derived hepatic tissue. A: The hepatocytes were immuno-marked by albumin, and co-located with nuclei by DAPI staining. Plots of semi-quantitative analysis of albumin fluorescent (red) signals. B: Quantitative analysis by flow cytometry. Plots presented as the ratio of the fluorescence intensity compared with control. Bar = 50 μm. $^{*}P < 0.05$ versus DMSO control. [Color figure can be viewed in the online issue, which is available at www.interscience.wiley.com.]

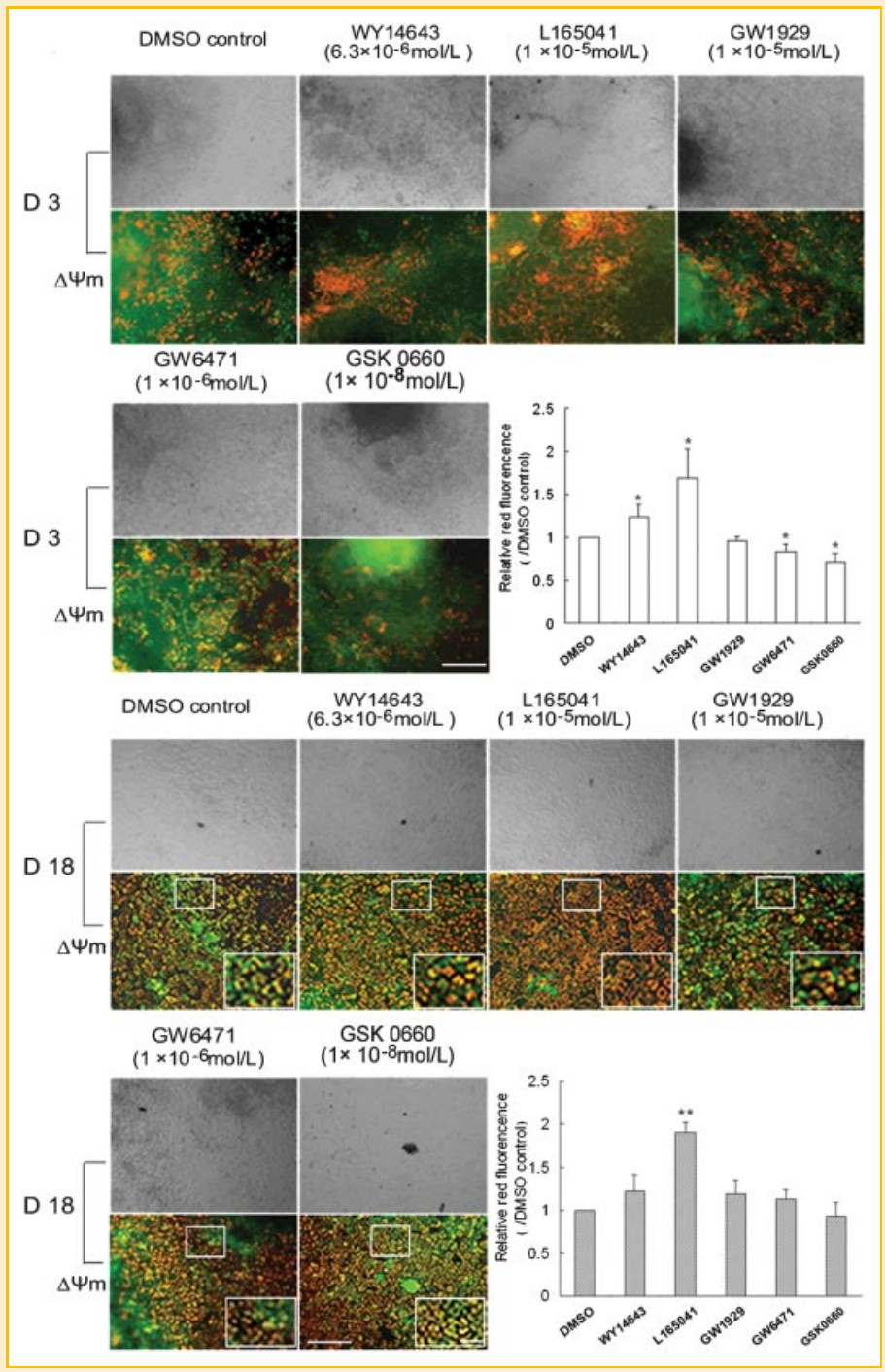

Fig. 4. Effects of PPARs agonists or antagonists on mitochondrial membrane potential ($\Delta\Psi_m$) formation in the ES cell-derived hepatic tissue. High $\Delta\Psi_m$ cells analyzed by JC-1 staining on D 3 and D 18. WY14643 is PPAR-α agonist, L165041 is PPAR-β agonist, GW1929 is PPAR-γ agonist, GW6471 is PPAR-α antagonist, and GSK0660 is PPAR-β antagonist. Plots of semi-quantitative analysis of red fluorescent signals in high $\Delta\Psi_m$ cells. The rectangular frames indicate the part magnified in panel. Bar = 50 μm, 10 μm (part magnified in the rectangular frames). $^{*}P < 0.05$, $^{**}P < 0.01$ versus DMSO control. [Color figure can be viewed in the online issue, which is available at www.interscience.wiley.com.]

in the magnitude and spatial distribution of high- and low-polarized mitochondria have been suggested to influence early embryo competence and [Müller-Höcker et al., 1996; Steuerwald et al., 2000; Van Blerkom et al., 2000; Reynier et al., 2001; Brenner et al., 2004]. Here we demonstrated the several elements of cellular energy metabolism, such as $\Delta\Psi_m$ and PPARs, in the hepatic-like tissue derived from mouse ES cells. Our results demonstrated that ES cells had the lowest mitochondrial mass and emitted almost only green fluorescence. In contrast, EBs showed both red and green fluorescence. The persistence of both fluorescences demonstrated

the presence of both high and low $\Delta\Psi_m$ coexisted inside EBs. Mitochondrial biogenesis is an adaptive biological process that occurs in response to developmental and physiologic cues. It has been demonstrated that mitochondrial oxidative phosphorylation was required for cardiac differentiation of stem cells [Chung et al., 2007]. Disruption of mitochondrial oxidative phosphorylation prevented stem cell differentiation into energetically competent. Within earlier differentiation period of myogenesis, cells switch from glycolytic metabolism to oxidative phosphorylation as the sources of ATP. There is a rapid increase in mitochondrial content, as indicated by an increase in mitochondrial volume [Moyes et al., 1997; Van Blerkom, 2008]. However, relatively little is known regarding mitochondriogenesis and mitochondrial function involved in ES cell derived hepatic-like tissue. The liver has high energy demand; the polarity ($\Delta\Psi_m$) is responsible for hepatocyte energetics and for apoptosis in pathobiology. The mitochondrial mass increase is associated with an enhancement in mitochondrial enzyme activity. High $\Delta\Psi_m$ and aerobic metabolism is a distinctive feature of fetal to adult hepatocyte transition [Sharma et al., 2006]. Mitochondria with red fluorescence represent mature and normal function [Lee et al., 2000; Sharma et al., 2006]. The number of cells with red fluorescence was counted as the mitochondrial numbers. In present study, there was an increase in active mitochondria mass with high $\Delta\Psi_m$ in red fluorescence from D 6 to D 18 during differentiation. On D 18, red fluorescence was almost observed all over the visual fields. It indicated that mitochondriogenesis started at EB formation, and the normal mitochondrial $\Delta\Psi_m$ was kept in the mature hepatic tissue on D 18. Meanwhile, we also have investigated the expression of PGC-1, which can be determined as one of the markers of the regulation of mitochondrial biogenesis [Wu et al., 1999]. PGC-1α expression took on an up regulating trend in the mitochondriogenesis. During this period, the undifferentiating mark OCT-4 was not expressed, the major phase II metabolism enzyme UGTs function and albumin expression were existed in the mature status. It implied that the proper mitochondrial function is a prerequisite during the course of hepatogenesis. Differences in the spatial distribution of high- and low polarized mitochondria in mouse and human oocytes and cleavage-stage embryos have been suggested to represent discrete regions of differential mitochondrial activity with distinct or focal regulatory functions [Van Blerkom et al., 2002; Van Blerkom, 2004]. The ES cells-derived hepatic tissue could be a valuable system for a variety of applications, including understanding the energy metabolism process.

Mitochondrial biogenesis requires coordinated changes in the metabolic enzymes of oxidative phosphorylation, TCA cycle, and fatty acid oxidation. PPARs serve as lipid-activated transcription factors that belong to the nuclear hormone receptor super-family. The differential expression and activation of PPARs during rat and mouse embryonic development, suggest that a period of PPARs exposure may be critical to normal development [Kliewer et al., 1994; Braissant and Wahli, 1998; Steinmetz et al., 2005]. However, the isotypes expressions in specific tissue development, such as embryonic liver, have not been investigated yet so far. Three PPAR isotypes, PPAR-α, PPAR-β, and PPAR-γ have been investigated here. All PPAR isoforms mRNA and proteins were expressed in different styles during the differentiation course, and PGC-1α took the almost same manner. For PPAR-α, it reached maximum expression on D 6, took on a down-regulating trend from D 12 to D 18. In contrast, the expression of PPAR-β exerted a rapidly elevated tendency during the later differentiation. As for PPAR-γ expression appeared low level and changed little before and after differentiation.

PPAR-β is the most ubiquitously expressed and appears very early during embryogenesis [Kliewer et al., 1994]. It has been linked to the embryo implantation. PPAR-β has a widespread distribution and is related with lipid metabolism and carbohydrate dynamic balance. The widespread expression of PPAR-β both in the embryo and in adult tissues suggests that the isoform may play a general "housekeeping" role [Han et al., 2005], even though its physiological and pathophysiological roles are less clear. PPAR-β can also inhibit inflammation, which may be important in liver [Burdick et al., 2006]. Additionally, PPAR-β is important in the liver for protecting against liver toxicity [Shan et al., 2008] and for regulating glucose homeostasis [Lee et al., 2006]. In present study, PPAR-β protein expression in fetal liver was higher than that in fetal heart, in concordance with previous report. During the course of differentiation, PPAR-β had an up-regulating trend by degrees with the maturation of hepatic-like tissue derived. Moreover, the expression level of PPAR-β was relatively higher than that of PPAR-α and PPAR-γ. The fluorescence merged area of PPAR-β with albumin was the largest, while PPAR-γ showed only weak fluorescence. The co-expressions of PPARs with albumin in the cells provided additional confirmation that only PPAR-β occupied the major position in energy metabolism of mature hepatocytes on D 18. Therefore, it seems that only PPAR-β takes an important role in energy metabolism of mature hepatocytes. The effect of PPAR-β agonist was to increase the number and size of albumin-positive hepatocytes, accelerate the mitochondriogenesis and maintain mitochondrial $\Delta\Psi_m$, which was determined by both immunocytochemistry assay and flow cytometry analysis. However, the maturation of hepatic-like tissue and mitochondriogenesis in hepatocyte could be efficiently abolished by PPAR-β specific antagonist GSK0660. It illuminated that PPAR-β agonist could enhance the differentiation of hepatic-like tissue. PPAR-β was involved in the development of hepatic tissue and may play a great role in the energy metabolism in the mature hepatic tissue. Furthermore, PPAR-β was necessary and important for mitochondriogenesis and mitochondrial $\Delta\Psi_m$ maintain during the hepatic tissue differentiation.

PPAR-α is mainly rich in tissues that have high energy demands, and serve as a key transcriptional regulator of the energy metabolic pathway [Leone et al., 1999]. As an important coactivator of PPAR-α, PGC-1α plays an important role in energy metabolism by coordinated transcriptional programs of mitochondrial biogenesis, adaptive thermogenesis and fatty acid β-oxidation. But in the hepatic differentiation case, both PPAR-α and PGC-1α only take a role at early stage. The results implied that ES cell-derived hepatocytes need the signals with a stronger energy demand at the early period of the hepatocytes formation. PPAR-α agonist was not affect albumin expression and mitochondrial $\Delta\Psi_m$ retention on D 18, although it could be accelerated by PPAR-α agonist and abolished by antagonist at the early stage.

PPAR-γ is predominantly expressed in intestine and adipose tissue where it triggers adipocyte differentiation and promotes lipid storage [Chawla et al., 1994]. During the course of ES cell-derived hepatic tissue differentiation, PPAR-γ kept a steady and low level. PPAR-γ agonist GW1929 showed no effect on albumin expression and mitochondrial $\Delta\Psi_m$ maintain on the phase of mature hepatic cells formation. Since PPAR-γ expression kept low level and remained unchanged on D 18, we did not consider to use its antagonist either.

In conclusion, the hepatic tissue derived morphologically possessed cellular energy metabolism features. PPAR-α and PGC-1α seemed only necessary for early mitochondriogenesis, but less important for $\Delta\Psi_m$ retention in the mature tissue derived. The enhanced co-expressions of PPARs and albumin, the effects of PPARs agonists or antagonists on hepatocytes maturation and mitochondriogenesis, as well as UGTs function with magnitude and spatial distribution of high- and low-polarized mitochondria further confirm that only PPAR-β took a role in cellular energy metabolism of hepatogenesis.

REFERENCES

Auboeuf D, Rieusset J, Fajas L, Vallier P, Frering V, Riou JP, Staels B, Auwerx J, Laville M, Vidal H. 1997. Tissue distribution and quantification of the expression of mRNAs of peroxisome proliferator-activated receptors and liver X receptor-alpha in humans: No alteration in adipose tissue of obese and NIDDM patients. Diabetes 46:1319–1327.

Bavister BD. 2006. The mitochondrial contribution to stem cell biology. Reprod Fertil Dev 18:829–838.

Braissant O, Wahli W. 1998. Differential expression of peroxisome proliferators-activated receptor-α, -β, and -γ during rat embryonic development. Endocrinology 139:2748–2754.

Brenner CA, Kubisch HM, Pierce KE. 2004. Role of the mitochondrial genome in assisted reproductive technologies and embryonic stem cell-based therapeutic cloning. Reprod Fertil Dev 16:743–751.

Brown GC. 1992. Control of respiration and ATP synthesis in mammalian mitochondria and cells. Biochem J 284:1–13.

Burdick AD, Kim DJ, Peraza MA, Gonzalez FJ, Peters JM. 2006. The role of peroxisome proliferator-activated receptor-beta/delta in epithelial cell growth and differentiation. Cell Signal 18:9–20.

Chawla A, Schwarz EJ, Dimaculangan DD, Lazar MA. 1994. Peroxisome proliferator-activated receptor (PPAR) γ: Adipose-predominant expression and induction early in adipocyte differentiation. Endocrinology 135:798–800.

Cho YM, Kwon S, Pak YK, Seol HW, Choi YM, Park do J, Park KS, Lee HK. 2006. Dynamic changes in mitochondrial biogenesis and antioxidant enzymes during the spontaneous differentiation of human embryonic stem cells. Biochem Biophys Res Commun 348:1472–1478.

Chung S, Dzeja PP, Faustino RS, Perez-Terzic C, Behfar A, Terzic A. 2007. Mitochondria oxidative metabolism is required for the cardiac differentiation of stem cells. Nat Clin Pract Cardiovasc Med 4:60–67.

Ding L, Liang XG, Zhu DY, Lou YJ. 2007. Peroxisome proliferator-activated receptor alpha is involved in cardiomyocyte differentiation of murine embryonic stem cells *in vitro*. Cell Biol Int 31:1002–1009.

Han S, Ritzenthaler JD, Wingerd B, Roman J. 2005. Activation of peroxisome proliferator-activated receptor β/δ (PPARβ/δ) increases the expression of prostaglandin E2 receptor subtype EP4. The roles of phosphatidylinositol 3-kinase and CCAAT/enhancerbinding protein beta. J Biol Chem 280:33240–33249.

Hellemans K, Michalik L, Dittie A, Knorr A, Rombouts K, De Jong J, Heirman C, Quartier E, Schuit F, Wahli W, Geerts A. 2003. Peroxisome proliferator-activated receptor-beta signaling contributes to enhanced proliferation of hepatic stellate cells. Gastroenterology 124:184–201.

Kliewer SA, Forman BM, Blumberg B, Ong ES, Borgmeyer U, Mangelsdorf DJ, Umesono K, Evans RM. 1994. Differential expression and activation of a family of murine peroxisome proliferators-activated receptors. Proc Natl Acad Sci USA 91:7355–7359.

Lee HC, Yin PH, Lu CY, Chi CW, Wei YH. 2000. Increase of mitochondria and mitochondrial DNA in response to oxidative stress in human cells. Biochem J 348:425–432.

Lee CH, Olson P, Hevener A, Mehl I, Chong LW, Olefsky JM, Gonzalez FJ, Ham J, Kang H, Peters JM, Evans RM. 2006. PPAR-δ regulates glucose metabolism and insulin sensitivity. Proc Natl Acad Sci USA 103:3444–3449.

Leone TC, Weinheimer CJ, Kelly DP. 1999. A critical role for the peroxisome proliferator-activated receptor alpha (PPAR alpha) in the cellular fasting response: The PPAR alpha-null mouse as a model of fatty acid oxidation disorders. Proc Natl Acad Sci USA 96:7473–7478.

Lim H, Dey SK. 2000. PPAR delta functions as a prostacyclin receptor in blastocyst implantation. Trends Endocrinol Metab 11:137–142.

Lonergan T, Brenner C, Bavister B. 2006. Differentiation related changes in mitochondrial properties as indicators of stem cell competence. J Cell Physiol 208:149–153.

Lonergan T, Bavister B, Brenner C. 2007. Mitochondria in stem cells. Mitochondrion 7:289–296.

Monica EK, Söderdahl T, Küppers-Munther B, Edsbahhe J, Andersson TB, Björquist P, Cotgreave I, Jernström B, Ingelman-Sundberg M, Johansson I. 2007. Expression of drug metabolizing enzymes in hepatocyte-like cells derived from human embryonic stem cells. Biochem Pharmacol 74:496–503.

Moyes CD, Mathieu-Costello OA, Tsuchiya N, Filburn C, Hansford RG. 1997. Mitochondrial biogenesis during cellular differentiation. Am J Physiol 272:1345–1351.

Müller-Höcker J, Schäfer S, Weis S, Münscher C, Strowitzki T. 1996. Morphological-cytochemical and molecular genetic analyses of mitochondria in isolated human oocytes in the reproductive age. Mol Hum Reprod 2:951–958.

Nadra K, Anghel SI, Joye E, Tan NS, Basu-Modak S, Trono D, Wahli W, Desvergne B. 2006. Differentiation of trophoblast giant cells and their metabolic functions are dependent on peroxisome proliferator-activated receptor beta/delta. Mol Cell Biol 26:3266–3281.

Ogawa S, Tagawa YI, Kamiyoshi A, Suzuki A, Nakayama J, Hashikura Y, Miyagawa S. 2005. Crucial roles of mesodermal cell lineages in a murine embryonic stem cell-derived in vitro liver organogenesis system. Stem Cells 23:903–913.

Oh SK, Kim HS, Ahn HJ, Seol HW, Kim YY, Park YB, Yoon CJ, Kim DW, Kim SH, Moon SY. 2005. Derivation and characterization of new human embryonic stem cell lines: SNUhES1, SNUhES2, and SNUhES3. Stem Cells 23:211–219.

Reynier P, May-Panloup P, Chrétien MF, Morgan CJ, Jean M, Savagner F, Barrière P, Malthièry Y. 2001. Mitochondrial DNA content affects the fertilizability of human oocytes. Mol Hum Reprod 7:425–429.

Schmelter M, Ateghang B, Helmig S, Wartenberg M, Sauer H. 2006. Embryonic stem cells utilize reactive oxygen species as transducers of mechanical strain-induced cardiovascular differentiation. FASEB J 20:1182–1184.

Shan W, Nicol CJ, Ito S, Bility MT, Kennett MJ, Ward JM, Gonzalez FJ, Peters JM. 2008. Peroxisome proliferator-activated receptor-beta/delta protects against chemically induced liver toxicity in mice. Hepatology 47:225–235.

Sharifpanah F, Wartenberg M, Hannig M, Piper HM, Sauer H. 2008. Peroxisome proliferator-activated receptor {alpha} agonists enhance cardiomyogenesis of mouse ES cells by utilization of a reactive oxygen species-dependent mechanism. Stem Cells 26:64–71.

Sharma NS, Shikhanovich R, Schloss R, Yarmush ML. 2006. Sodium butyrate treated embryonic stem cells yield hepatocyte-like cells expressing a glycolytic phenotype. Biotechnol Bioeng 94:1053–1063.

Shearer BG, Steger DJ, Way JM, Stanley TB, Lobe DC, Grillot DA, Iannone MA, Lazar MA, Willson TM, Billin AN. 2008. Identification and characterization of a selective peroxisome proliferator-activated receptor β/δ (NR1C2) antagonist. Mol Endocrinol 22:523–529.

Sher T, Yi HF, McBride OW, Gonzalez FJ. 1993. cDNA cloning, chromosomal mapping, and functional characterization of the human peroxisome proliferator activated receptor. Biochemistry 32:5598–5604.

Shi Q, Lou YJ. 2005. Microsomal glutathione transferase 1 is not S-nitrosylated in rat liver microsomes or in endotoxin challenged rats. Pharmacol Res 51:303–310.

Squirrell JM, Schramm RD, Paprocki AM, Wokosin DL, Bavister BD. 2003. Imaging mitochondrial organization in living primate oocytes and embryos using multiphoton microscopy. Microsc Microanal 9:190–201.

St John JC, Ramalho-Santos J, Gray HL, Petrosko P, Rawe VY, Navara CS, Simerly CR, Schatten GP. 2005. The expression of mitochondrial DNA transcription factors during early cardiomyocyte *in vitro* differentiation from human embryonic stem cells. Cloning Stem Cells 7:141–153.

Steinmetz M, Quentin T, Poppe A, Paul T, Jux C. 2005. Changes in expression levels of genes involved in fatty acid metabolism: Upregulation of all three members of the PPAR family (alpha, gamma, delta) and the newly described adiponectin receptor 2, but not adiponectin receptor 1 during neonatal cardiac development of the rat. Basic Res Cardiol 100:263–269.

Steuerwald N, Barritt JA, Adler R, Malter H, Schimmel T, Cohen J, Brenner CA. 2000. Quantification of mtDNA in single oocytes, polar bodies and subcellular components by real-time rapid cycle fluorescence monitored PCR. Zygote 8:209–215.

Tsutsui M, Ogawa S, Inada Y, Tomioka E, Kamiyoshi A, Tanaka S, Kishida T, Nishiyama M, Murakami M, Kuroda J, Hashikura Y, Miyagawa S, Satoh F, Shibata N, Tagawa Y. 2006. Characterization of cytochrome P450 expression in murine embryonic stem cell-derived hepatic tissue system. Drug Metab Dispos 34:696–701.

Van Blerkom J. 2004. Mitochondria in human oogenesis and preimplantation embryogenesis: Engines of metabolism, ionic regulation and developmental competence. Reproduction 28:269–280.

Van Blerkom J. 2008. Mitochondria as regulatory forces in oocytes, preimplantation embryos and stem cells. Reprod Biomed Online 16: 553–569.

Van Blerkom J, Davis P, Alexander S. 2000. Differential mitochondrial distribution in human pronuclear embryos leads to disproportionate inheritance between blastomeres: Relationship to microtubular organization. ATP content and competence. Hum Reprod 15:2621–2633.

Van Blerkom J, Davis P, Mathwig V, Alexander S. 2002. Domains of high-polarized and low-polarized mitochondria may occur in mouse and human oocytes and early embryos. Hum Reprod 17:393–406.

Willson TM, Brown PJ, Sternbach DD, Henke BR. 2000. The PPARs: From orphan receptors to drug discovery. J Med Chem 43:527–550.

Wu Z, Puigserver P, Andersson U, Zhang C, Adelmant G, Mootha V, Troy A, Cinti S, Lowell B, Scarpulla RC, Spiegelman BM. 1999. Mechanisms controlling mitochondrial biogenesis and respiration through the thermogenic coactivator PGC-1. Cell 98:115–124.

Zhu DY, Du Y, Huang X, Guo MY, Ma KF, Yu YP, Lou YJ. 2008. MAPEG expression in murine embryonic stem cell-derived hepatic tissue system. Stem Cells Dev 17:775–784.

Zuliani T, Duval R, Jayat C, Schnébert S, André P, Dumas M, Ratinaud MH. 2003. Sensitive and reliable JC-1 and TOTO-3 double staining to assess mitochondrial transmembrane potential and plasma membrane integrity: Interest for cell death investigations. Cytometry A 54:100–108.